JOC The Journal of Organic Chemistry

Article

pubs.acs.org/joc

Theoretical Study of the BF_3-Promoted Rearrangement of Oxiranyl *N*-Methyliminodiacetic Acid Boronates

Margarita M. Vallejos*,† and Silvina C. Pellegrinet*,‡

†Laboratorio de Química Orgánica, IQUIBA-NEA, Universidad Nacional del Nordeste, CONICET, FACENA, Av. Libertad 5460, Corrientes 3400, Argentina

‡Instituto de Química Rosario (CONICET), Facultad de Ciencias Bioquímicas y Farmacéuticas, Universidad Nacional de Rosario, Suipacha 531, Rosario 2000, Argentina

Supporting Information

ABSTRACT: The mechanism of the rearrangement of oxiranyl *N*-methyliminodiacetyl (MIDA) boronates in dichloromethane has been extensively investigated with density functional theory. Several reaction pathways were examined. Our results revealed that the most-favorable mechanisms for the BF_3-promoted rearrangement of 2-phenyl oxiranyl MIDA boronate (**1**) and 1-phenyl oxiranyl MIDA boronate (**24**) comprise two steps: ring opening of the epoxide to a carbocation intermediate followed by migration of a MIDA-boryl group (for the reaction of **1**) and hydrogen (for the reaction of **24**), to give the same BF_3-coordinated α-boryl aldehyde in both cases. The first step of the ring opening of the epoxide is the rate-determining step of these reactions. In the rearrangement step for the reaction of **1**, the MIDA-boryl group migrates easily, probably because of its electron-rich sp^3-hybridized boron center. For **24**, the most-favorable pathway involves a rare boryl-substituted carbocation. The course of these reactions is mainly controlled by electronic effects, although steric effects are also significant. The higher energy barrier calculated for the unsubstituted oxiranyl MIDA boronate (**31**) explains the lack of reactivity in the studied BF_3-promoted rearrangement.

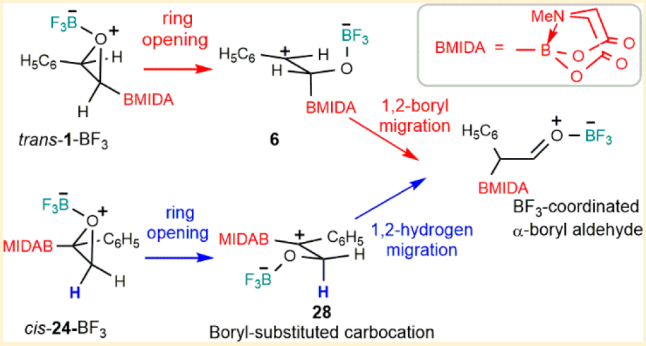

INTRODUCTION

Epoxides are useful intermediates in organic synthesis because of their availability and ease of transformation into a wide variety of valuable compounds.[1−7] One of the most useful transformations of epoxides is their Lewis acid-catalyzed rearrangement to give carbonyl compounds.[8−12]

In recent years, Burke and co-workers[13,14] have discovered a new class of stable compounds that have the tetracoordinated *N*-methyliminodiacetyl (MIDA) boryl group. It was demonstrated that vinyl-MIDA boronates undergo epoxidation with *m*-CPBA to provide oxiranyl MIDA boronates.[13,15] In addition, Yudin and co-workers[16] have reported that the BF_3-promoted rearrangement of 2-substituted oxiranyl MIDA boronates (R = alkyl or aryl groups) in DCM, warming from −30 to 0 °C over 30 min generates the corresponding α-boryl aldehydes as unique products in high yields. Also, no ketone byproducts are obtained (Scheme 1). However, the reaction does not proceed with the unsubstituted oxiranyl MIDA boronate (R = H), even at a higher temperature and longer reaction time (40 °C, 24 h). Interestingly, the same α-boryl aldehyde is obtained by the BF_3-promoted rearrangement of both 1- and 2-substituted oxiranyl MIDA boronate (R = Ph) (Scheme 1).

The reactions of 1-deuterated oxiranyl MIDA boronates with BF_3 have been carried out to gain insight about their mechanism and regioselectivity.[16] The outcome of these experiments showed that the deuterium label is placed at the carbonyl carbon of the α-boryl aldehyde, suggesting that an unusual 1,2-boryl shift occurs. On the basis of experimental results, Yudin and co-workers also suggested that the reaction of 1-substituted oxiranyl MIDA boronates might take place via a 1,2-hydride migration.

In a contemporary work, Burke and co-workers reported a similar rearrangement of oxiranyl pinene-derived iminodiacetic acid (PIDA) boronates promoted by magnesium perchlorate, $Mg(ClO_4)_2$, to yield stable α-boryl aldehydes through 1,2-boryl migration with complete maintenance of the stereochemical purity, demonstrating the stereospecificity of this transformation.[17]

The rearrangement of oxiranyl MIDA boronates is a valuable synthetic method for preparing α-boryl aldehydes, which have

Scheme 1

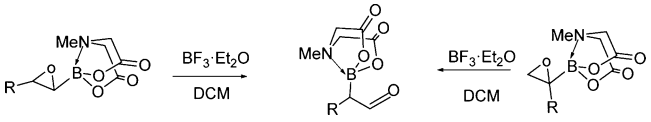

Received: May 5, 2017
Published: May 11, 2017

DOI: 10.1021/acs.joc.7b01096
J. Org. Chem. 2017, 82, 5917−5925

shown great versatility as building blocks in the synthesis of a large variety of functionalized organoboron compounds.[18−25]

Several theoretical studies have been conducted to achieve more understanding about the mechanism of the rearrangement of epoxides. It has been reported that ring opening of 2,2-dimethyloxirane[10] and 2-*tert*-butyl-2-methyloxirane[26] catalyzed by a Lewis acid such as BF_3 occurs by a stepwise mechanism via a zwitterionic intermediate. The formation of a BF_2-bound fluorohydrin was also suggested as a competing mechanism.

More recently, Salvatella and co-workers[27] investigated the possible mechanisms of the BF_3-catalyzed Meinwald rearrangement for a wide range of epoxides. These authors proposed, as plausible reaction pathways, a concerted mechanism and three stepwise mechanisms via formation of a zwitterionic intermediate, a BF_3-addition compound, or both, with all paths involving epoxide ring opening, C−C bond rotation, and alkyl or hydrogen migration.

In this work, we have performed a theoretical study of the BF_3-promoted rearrangement of 2- and 1-phenyl-substituted and unsubstituted oxiranyl MIDA boronates (Figure 1), in order to provide a detailed understanding about the reaction mechanisms. To our knowledge, no report on the theoretical study of the mechanism of the BF_3-promoted rearrangement of epoxides bearing a BMIDA group has been described to date, particularly in regards to the unprecedented 1,2-boryl migration. In addition, we wanted to rationalize the experimental regioselectivity and reactivity for such reactions.

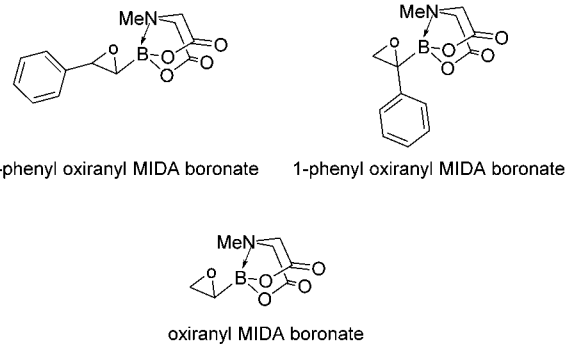

Figure 1. Studied oxiranyl MIDA boronates.

COMPUTATIONAL METHODS

We initially performed thorough conformational searches to locate the lowest-energy geometries of the chemical species under study. Final-geometry optimizations were carried out using the MPWB1K[28] global hybrid meta-GGA functional together with the 6-311G* basis set. The MPWB1K functional proposed by the Truhlar group has been found to provide an improvement in the accuracy of the thermodynamic data in excellent agreement with experimental results.[29−31]

Frequency calculations were performed to determine the nature of the stationary points: the transition structures (TSs) had one imaginary frequency, and the reactants, the intermediate structures, and the products had no imaginary frequencies. Solvent effects in DCM (solvent used experimentally) were taken into account through full optimizations using the SMD-continuum solvation method.[32] Free energies were computed at 298.15 K and 1 atm in DCM.

To verify the connectivity of the TSs with the correct local minima, intrinsic reaction coordinates (IRCs) were computed from every optimized TS in forward and reverse directions along the imaginary mode of vibration using either the Hessian-based predictor corrector (HPC)[33,34] or the local quadratic approximation (LQA)[35,36] algorithms.

Bond orders (Wiberg Bond indices, WBIs)[37] and atomic charges were calculated with the natural bond orbital (NBO)[38,39] method. All computations were carried out with the Gaussian 09 suite of programs.[40]

RESULTS AND DISCUSSION

Rearrangement of the Complex 2-Phenyl-oxiranyl MIDA Boronate-BF_3. The reaction pathways calculated for the BF_3-promoted rearrangement of 2-phenyl oxiranyl MIDA boronate (**1**) are shown in Figures 2 and 3, respectively.

Complexation between **1** and BF_3 may occur on either face of the epoxide, giving two reactive-complexes *trans*-**1**-BF_3 and *cis*-**1**-BF_3,[41] the second being less stable by 1.0 kcal/mol, due to the steric clashes between the BMIDA and BF_3 groups.

The energies of the reactive complexes are considerably lower than the total energy of separate reactants because of favorable complexation. For this reason, relative free energies were computed from the most-stable reactive complex (*trans*-**1**-BF_3).

Each reactive complex can undergo two alternative ring-opening paths, through the rupture of the C2−O (Figure 2) or C1−O (Figure 3) bonds. The ring-opening process is accompanied by C1−C2 bond rotation,[10] so two routes are feasible. They involve the C−O bond approaching either the less or more bulky group, which we have named *anti*/*syn* pathways.

Rupture of the C2−O Bond. Reactive-complexes *trans*-**1**-BF_3 and *cis*-**1**-BF_3 may undergo *anti* and *syn* pathways through the two-step mechanism involving a carbocation intermediate. The first step of the *anti* pathways occur through TSs **2** and **4**, in which the C1−O bond is close to H_b, leading to zwitterion intermediates **6** and **8**, respectively. TS **2** (9.5 kcal/mol) is energetically more favorable than TS **4** (14.8 kcal/mol) because of less steric hindrance between the OBF_3 group and BMIDA moiety, which is in line with the relative energies of the starting reactive complexes. Intermediates **6** and **8** undergo C1−O bond rotation and BMIDA migration with very low activation barriers (4.8 and 0.4 kcal/mol) through TSs **10** and **12**, respectively. In TSs **10** and **12**, the BMIDA group is almost aligned with the *p*-orbital of the nearly planar C2, showing imaginary frequencies that correspond to the shift of the BMIDA group from C1 to C2. Then, TSs **10** and **12** lead to the BF_3-α-borylaldehyde products in *exo* **14**-X and *endo* **14**-N conformations, respectively, with the former being more stable by 3.3 kcal/mol.[42]

The *syn* routes involve TSs **3** and **5**, in which C1−O is close to the phenyl group. Again, TS **3** is more stable than TS **5** by 2.4 kcal/mol because of the steric hindrance of the starting reactive complex. TS **3** leads to a stable zwitterion intermediate **7** (−3.3 kcal/mol) and TSs **5** yields **9** (5.5 kcal/mol). Intermediate species **7** and **9** undergo a H_a shift through TSs **11** and **13** to form BF_3-coordinated MIDA acylboronate products **15**-N (−19.2 kcal/mol) and **15**-X (−16.4 kcal/mol), respectively. Such compounds have been obtained as air-stable solids through Dess−Martin oxidation of α-hydroxyboronates.[43]

To explain the preference of BMIDA migration relative to hydrogen migration, we have analyzed the more favorable pathways. The geometrical data, WBIs, and natural charges of the TSs are displayed in the Supporting Information.

The activation barrier of the first step of the *anti*-pathway (through TS **2**) is 4.3 kcal/mol lower than that of the *syn*-pathway (through TS **3**). In TS **2**, the atoms C3−C2−C1−H_a

DOI: 10.1021/acs.joc.7b01096
J. Org. Chem. 2017, 82, 5917−5925

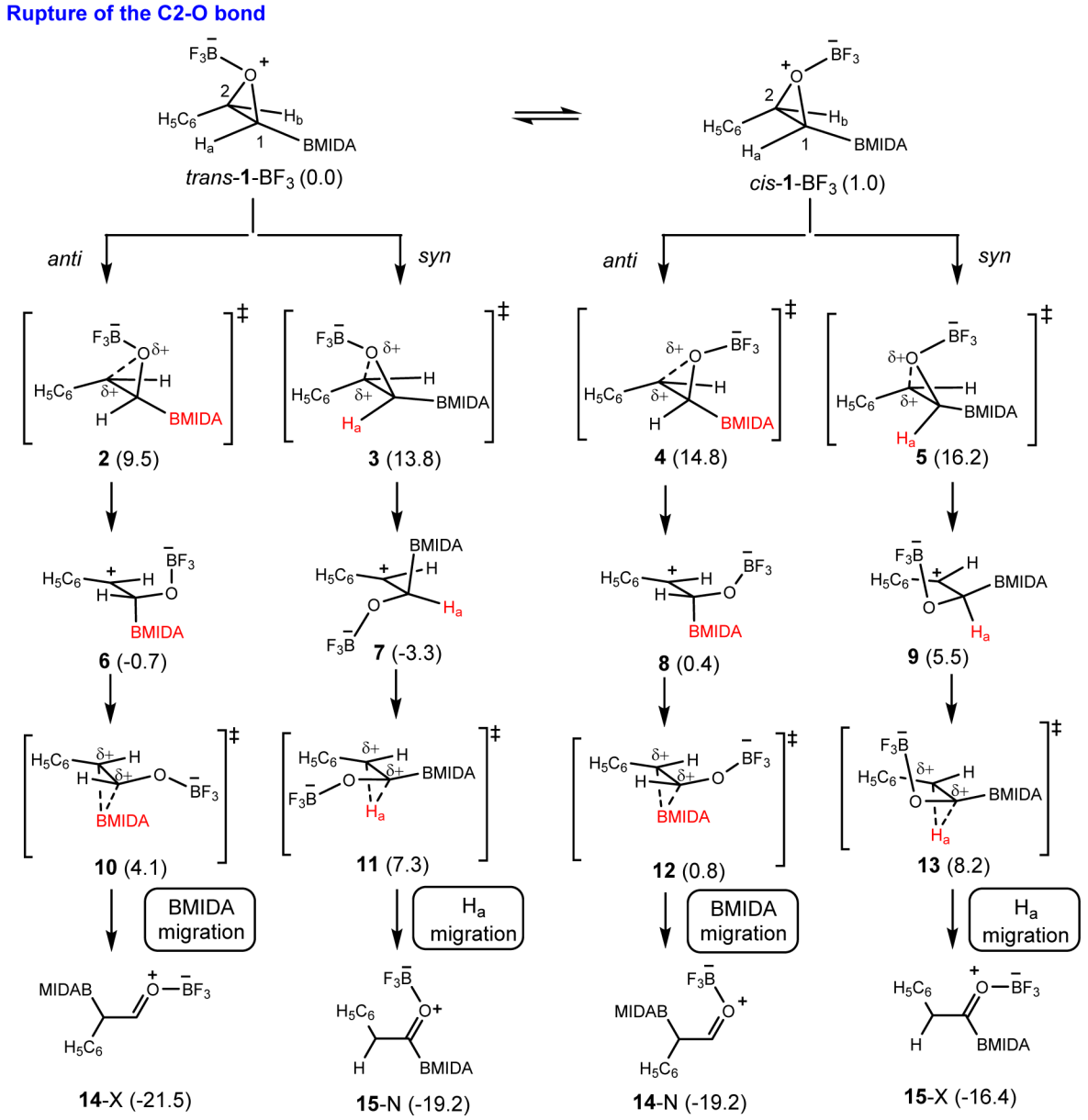

Figure 2. Reaction pathways of the rearrangement of the BF_3-coordinated 2-phenyl oxiranyl MIDA boronate with rupture of the C2−O bond. Relative Gibbs free energies in DCM are given in parentheses (in kcal/mol).

are almost in the same plane (13.2°, *syn*-periplanar) and in TS **3** the atoms C3−C2−C1−B(MIDA) show an *anti*-periplanar arrangement (178.4°). In TS **2**, the C1−H_a bond is nearly eclipsed with the phenyl group while in TS **3** the C2−H_b bond is eclipsing the BMIDA group; hence, **3** is more sterically congested. In both TSs, the C2−C3 distance is shorter (1.39 Å in TS **2** and 1.38 Å in TS **3**), and the WBI between C2 and C3 atoms is higher (1.334 in TS **2** and 1.437 in TS **3**) than in *trans*-**1**-BF_3 (d = 1.47 Å and WBi = 1.003), indicating a substantial C2−C3 double bond character because of the resonance effect. The charges at the C1 and C2 atoms are −0.256 and +0.254 e in TS **2**, and −0.271 and +0.261 e in TS **3**, respectively, which denotes the delocalization of charges to stabilize the carbocation C2, being more notable in TS **2**. Thus, the greater stability of TS **2** relative to TS **3** is mainly attributed to steric effects, although the greater charge delocalization also provides more stability.

TS **10**, associated with the shift of the BMIDA group, has a smaller activation barrier than TS **11** for H_a migration (4.8 and 10.6 kcal/mol, respectively). In TS **10**, the atoms C3−C2−C1−O show an *anti*-periplanar arrangement (169.5°). However, in TS **11** they are in a *syn*-periplanar layout (4.8°), and the phenyl group is twisted out of the plane to relieve the van der Waals interaction with the OBF_3 group.

The structures of TS **10** and **11** allow the delocalization of charges because of the resonance effect, being more favorable in the former, and as a consequence the C1−O, C1−C2, and C2−C3 bonds are shorter in these TSs than in *trans*-**1**-BF_3.

In TS **10**, the bond distances and WBIs of C1−B(MIDA) (d = 1.90 Å, WBI = 0.410) and C2−B(MIDA) (d = 2.20 Å, WBI = 0.198), and in TS **11**, the bond distances and WBIs for C1−H_a (d = 1.22 Å, WBI = 0.520) and C2−H_a (d = 1.47 Å, WBI = 0.266) indicate that bond breaking/forming is occurring, respectively, and also that migration is more advanced in TS **10** than TS **11**.

DOI: 10.1021/acs.joc.7b01096
J. Org. Chem. 2017, 82, 5917−5925

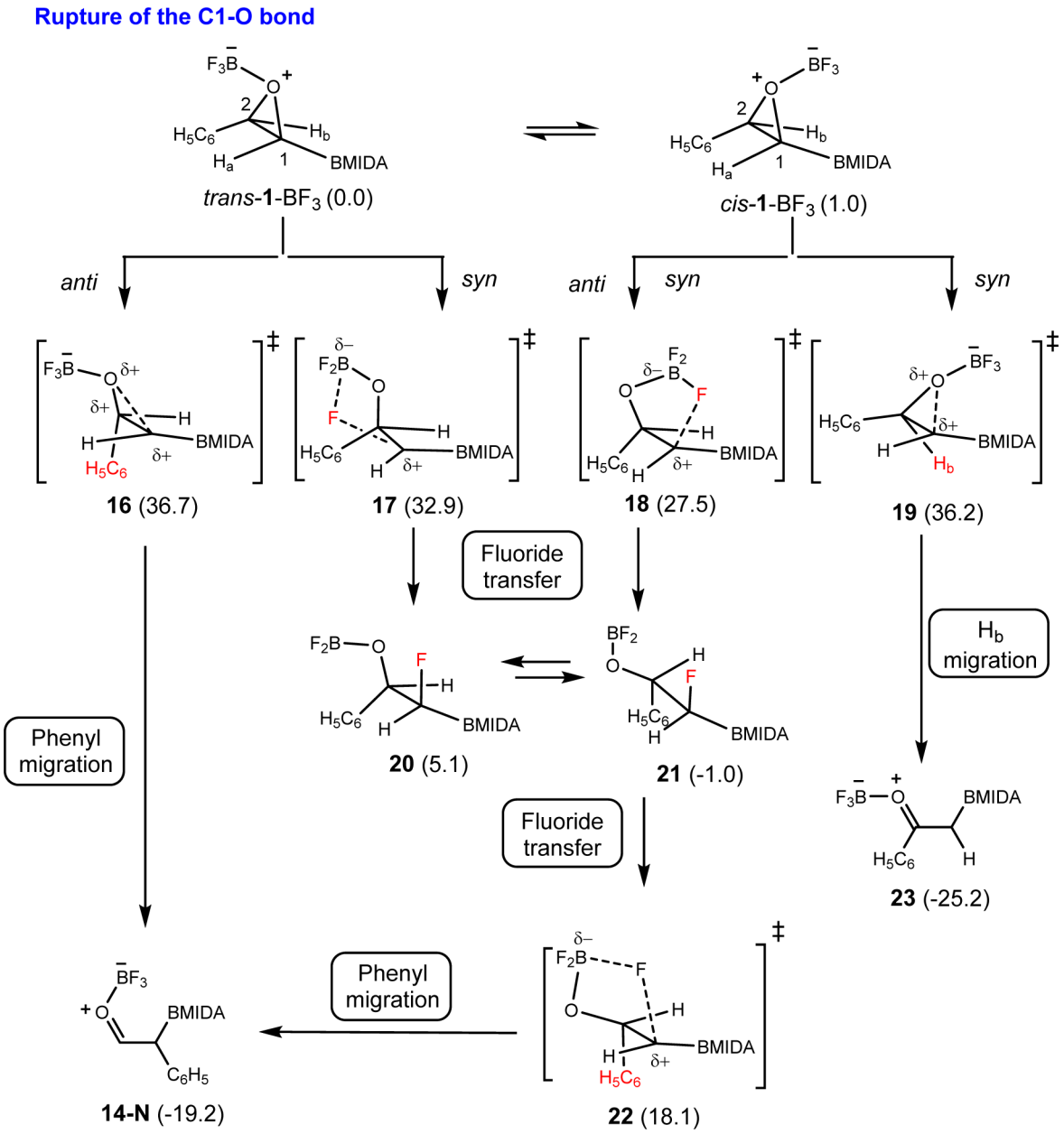

Figure 3. Reaction pathways of the rearrangement of the BF_3-coordinated 2-phenyl oxiranyl MIDA boronate with rupture of the C1−O bond. Relative Gibbs free energies in DCM are given in parentheses (in kcal/mol).

The B(MIDA) (+1.283 *e*) and H_a (+0.362 *e*) atoms in TS **10** and TS **11** become more positive than in reactive complexes and more positive than in TS **2** and TS **3**, respectively. In addition, both the C1/C2 atoms lose/gain electron population, respectively. However, whereas in TS **10**, C1 and C2 become positive (+0.014 *e*)/negative (−0.038 *e*) respectively; in TS **11**, C1 and C2 atoms are less negative (−0.050 *e*)/positive (+0.029 *e*) than in the reactive complex and than in TS **3**. Thus, the ease of migration showed by the BMIDA group is attributed to its electron-rich sp^3-hybridized boron center, which imparts more stability.

Rupture of the C1−O Bond. The ring opening of *trans*-**1**-BF_3 and *cis*-**1**-BF_3 is accompanied by the movement of C1−C2, with C2−O approaching H_a (*anti* path) or the BMIDA group (*syn* path) (Figure 3).

The concerted mechanisms may occur via TS **16** and TS **19** following *anti* and *syn* paths, from *trans*-**1**-BF_3 and *cis*-**1**-BF_3 respectively. The *anti* pathway (through TS **16**) involves a phenyl migration to generate **14-N**, whereas the *syn* route undergoes hydrogen (H_b) migration (through TS **19**) to yield ketone **23**.

Product **23** is more stable than **14-X**, however TSs **16** (36.7 kcal/mol) and **19** (35.2 kcal/mol) have higher energy barriers than the TSs in which the rupture of the C2−O bond occurs. Thus, the reaction appears to be kinetically controlled.

Trans-**1**-BF_3 and *cis*-**1**-BF_3 may also follow *syn* or *anti* pathways via TSs **17** and **18**, respectively. In TSs **17** and **18**, ring opening is accompanied by rotation of OBF_3 group around the C1−C2 bond, placing a fluorine in a favorable position to interact with the incipient carbocation at C1 (C1−F = 2.30 and 2.44 Å for **17** and **18**). Fluoride transfer from the BF_3 group to C1 occurs, leading to BF_2-bound fluorohydrin intermediates **20** and **21** (through TSs **17** and **18**, respectively). The energy barriers associated with TSs **17** (32.9 kcal/mol) and **18** (26.5

DOI: 10.1021/acs.joc.7b01096
J. Org. Chem. 2017, 82, 5917−5925

kcal/mol) are also higher than those corresponding to the ring opening at the C2−O bond, but they are lower than TSs **16** and **19**, which is attributed to the stabilizing interaction $F_2BF\cdots$ C1. Similar mechanisms for the formation of BF_3-addition compounds have been reported for the reaction of some epoxides with BF_3.[44−49]

BF_2-bound fluorohydrin **20** shows an eclipsed conformation and has a higher free energy (5.1 kcal/mol) than its *anti*-analogue **21** (−1.0 kcal/mol). Conformer **20** could generate **21** by rotation of the C1−C2 bond, and then follow the same reaction path. In TS **22** (18.1 kcal/mol), the phenyl group is favorably placed for migration and then leads to **14-N**.

The reaction pathways that involve ring opening at C1−O bond are less favorable, because the carbocation formed is not stabilized by resonance as in the case of the reaction routes that involve rupture at C2−O bond.

The changes in C1−C2 bond distances and WBI are not noticeable, and the C2−C3 bond is longer in TSs **16** and **19** relative to the corresponding starting reactive complexes because of the lack of resonance effect. The charge on C1 becomes positive in both TSs (+0.161 *e* in TS **16** and +0.249 *e* in TS **19**) and the charge on C2 is less positive in TS **16** (+0.041 *e*). Also, it is slightly negative in TS **19** (−0.013 *e*). In TSs **17** and **18**, although there are stabilizing interactions C1$\cdots$F, the lack of resonance is dominant in the higher energy barriers.

All these calculations suggest that the most favorable pathway for the studied rearrangement comprises a two-step mechanism that involves rupture of the C_2−O bond via TS **2** to give carbocation **6** followed by B(MIDA) group migration via TS **10**, which yields *α*-borylaldehyde **14-X** as the unique product, which is in agreement with experimental results (Figure 4).[16] The regioselectivity of this reaction is mainly controlled by electronic factors.

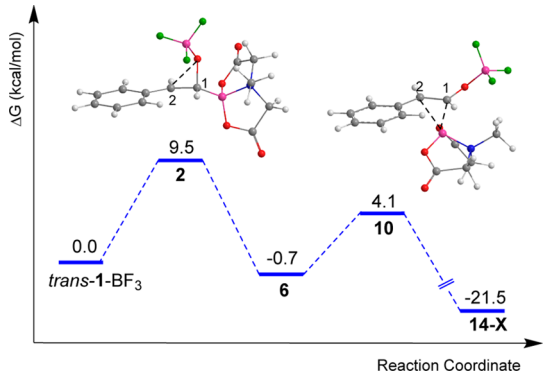

Figure 4. Reaction profile for the most-favorable pathway of BF_3-promoted rearrangement of 2-phenyl oxiranyl MIDA boronate (**1**). Optimized geometries of the TSs **2** and **10** are shown.

Rearrangement of BF_3-Coordinated 1-Phenyl Oxiranyl MIDA Boronate. The mechanisms computed for the reaction of BF_3-coordinated 1-phenyl oxiranyl MIDA boronate (**24**) considering the ring opening at the most substituted bond (C1−O) are gathered in Figure 5. The rupture of the less-substituted bond (C2−O) is predicted to occur with a much higher energy barrier (between 32 to 48 kcal/mol) because of the lack of the stabilizing resonance effect, as was also demonstrated for the rearrangement of BF_3-coordinated oxiranyl boronate **1** (see the Supporting Information).

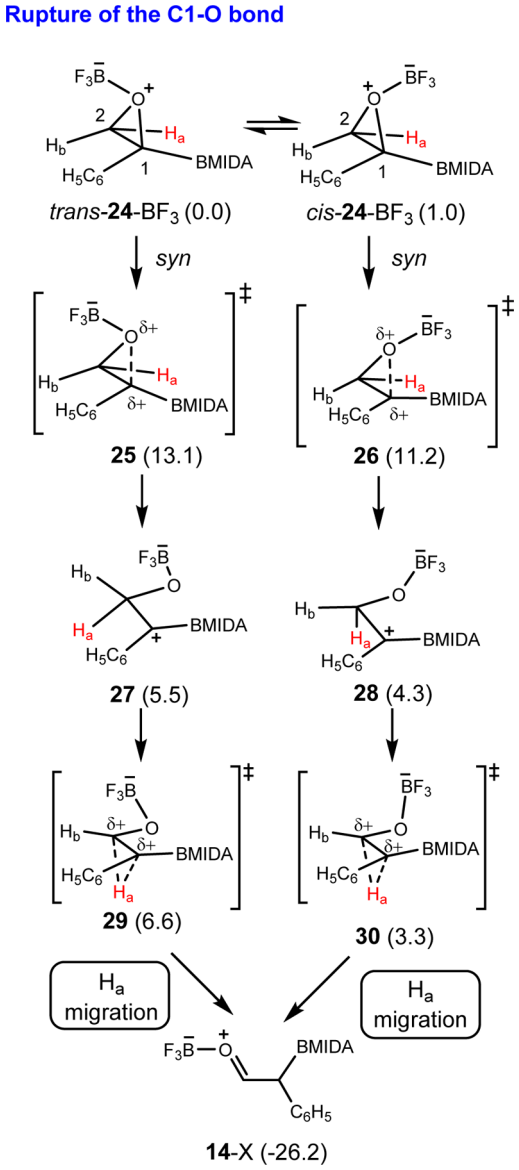

Figure 5. Reaction pathways of the rearrangement of the BF3-coordinated 1-phenyl oxiranyl MIDA boronate with rupture of the C1−O bond. Relative Gibbs free energies in DCM are given in parentheses (in kcal/mol).

Complexation between BF_3 and **24** leads to two reactive-complexes *trans*-**24**-BF_3 and *cis*-**24**-BF_3,[41] the second being less stable than the former conformer by 1.0 kcal/mol.

The ring opening of each reactive complex is accompanied by the C1−C2 bond rotation, and we were able to find two possible *syn* pathways in which the C−O bond is close to the BMIDA group. Attempts to find TSs for *anti* pathways, in which the C−O bond is close to the phenyl group, were unsuccessful. This is presumably because of the more-constrained rotation of C2-OBF_3 group toward the phenyl group.

The reaction pathways involve two-step mechanisms; first, the ring opening occurs via TSs **25** and **26**, which lead to zwitterion intermediates **27** and **28**, and then hydrogen migration (H_a) takes place through TSs **29** and **30**, respectively. Both paths lead to the BF_3-coordinated *α*-boryl aldehyde **14-X**, as was obtained in the most-favorable mechanism of the

DOI: 10.1021/acs.joc.7b01096
J. Org. Chem. 2017, 82, 5917−5925

rearrangement of **1**, and in agreement with the experimental results.

The first step of these mechanisms is the rate-limiting step. The energy barrier for TS **25** (13.1 kcal/mol) is higher than that for TS **26** (10.2 kcal/mol). In TSs **25** and **26**, C1, C2, B, and the atoms of phenyl group are almost in the same plane. In TS **25**, the OBF_3 group is closer to the phenyl group, and the atoms C3−C1−C2−H_b show a nearly *syn*-periplanar arrangement (8.1°). In TS **26**, the OBF_3 group is placed away from the BMIDA group to relieve the steric tension between both groups ,and thus, this structure is less congested than TS **25**. Also, in TS **26** H_a and H_b are similarly placed: relative to the vacant *p* orbital of C1, and appear to have an equal tendency to migrate, whereas in TS **25** only H_a is in a better position to migrate.

In both TSs, a redistribution of the charge density occurs as a consequence of the rupture of C1−O bond. The charges of C1/C2 become positive/negative in TSs **25** and **26** (C1= +0.091 and +0.141 *e* and C2 = −0.059 and −0.063 e for TSs **25** and **26**, respectively). The positive charge on the carbocation C1 is delocalized by resonance, causing a decrease of the C1−C3 bond distance in TSs **25** and **26** (1.43 and 1.44 Å, respectively) relative to the corresponding starting reactive complexes (1.49 Å). Thus, in both TSs the resonance effect stabilizes the incipient carbocation; the lowest energy barrier for TS **26** is mainly attributed to its lesser steric hindrance.

The free energies of TSs **29** and **30** are very similar to those for intermediates **27** and **28** (1.1 kcal/mol higher and 1.0 kcal/mol lower, respectively), so this step is predicted to be essentially barrierless. The hydrogen shift is significantly advanced in TSs **29** and **30**; C2−H_a is almost aligned with the *p*-orbital of C1, and shows an increase in bond length (1.18 and 1.16 Å, respectively). Also, the C1−C2 bond distance decreases and its WBI increases in both TSs **29** and **30** (1.41 Å and 1.251 for TS **29** and 1.42 Å and 1.234 for TS **30**), showing partial double-bond character, which is due to the charge redistribution. The charges of H_a and C1 become more positive/slightly less positive in TSs **29** and **30** relative to those in TS **25** and **26**, respectively.

Thus, even though both pathways lead to the expected product **14-X**, the mechanism starting from *cis*-**24**-BF_3, depicted in Figure 6, is more probable to occur. The energy profile is comparable to that of the most-favorable route for the rearrangement of **1**. Another crucial point is that in contrast to 2-phenyl oxiranyl MIDA boronate (**1**), for 1-phenyl oxiranyl MIDA boronate (**24**) we were able to locate boryl-substituted carbocations such as **27** and **28**. The presence of a stabilizing substituent such as a phenyl group on the positive carbon seems to determine whether such unusual cationic species can be formed or not and therefore whether migration and epoxide ring opening proceed in a stepwise or concerted fashion.

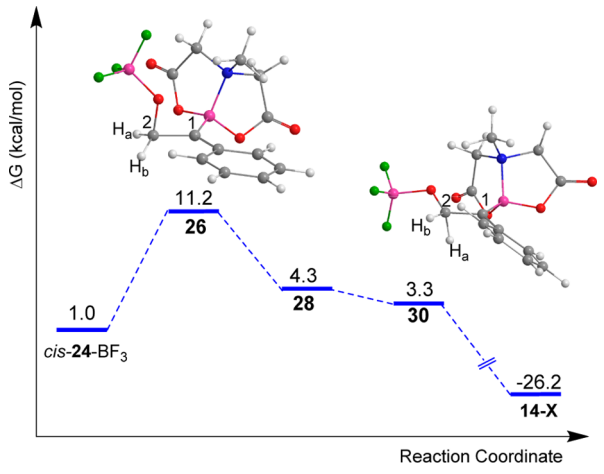

Figure 6. Reaction profile for the most-favorable pathway of BF_3-promoted rearrangement of 1-phenyl oxiranyl MIDA boronate (**24**). Optimized geometries of the TSs **26** and **30** are shown.

Rearrangement of BF_3-Coordinated Oxiranyl MIDA Boronate. The mechanisms calculated for the rearrangement of BF_3-coordinated oxiranyl MIDA boronate (**31**) are shown in Figures 7 and 8. Two reactive complexes are obtained by interaction of **31** with BF_3, *trans*-**31**-BF_3, and *cis*-**31**-BF_3, the latter being less stable by 4.6 kcal/mol, because of its higher steric hindrance between the BF_3 and BMIDA groups.

Rupture of the C2−O Bond. For this mechanism, when the C−O bond is close to H_c/H_b, the pathways are called *anti* and *syn*, respectively. The ring opening at the C2−O bond for the *anti* and *syn* pathways from *trans*-**31**-BF_3, and the *anti* pathway from *cis*-**31**-BF_3, involve a concerted mechanism in which 1,2-boryl migration occurs through TSs **32**−**34** (Figure 7).

In TS **32**, the atoms H_a−C1−C2−H_b have an almost *anti*-periplanar arrangement (176°) and C_2−C_1−B(MIDA) forms an angle of 116°, indicating that the boryl group is placed to migrate. In TS **33**, the H_a is placed more favorably to migrate (C2−C1−H_a = 112°). However, the IRC calculation leads to the final product through a 1,2-boryl shift. In TS **34** the BMIDA group is placed favorably to migrate as in TS **32**, but BF_3 is on the same side of the BMIDA group (relative to starting reactive complex), resulting in greater steric hindrance and thus a less stable TS (40.6 kcal/mol).

TSs **32** and **33** lead to *exo* BF_3-coordinated α-boryaldehyde **38-X** (−27.4 kcal/mol), which is more stable than its *endo* form **38-N** (−24.6 kcal/mol), obtained through TS **34**.

Rearrangement of *cis*-**31**-BF_3 along the *syn* route is accompanied by rotation about C1-OBF_3, which favorably positions a fluorine of BF_3 (C2−F = 2.28 Å) to interact with the C2 atom in TS **35**. The fluoride transfer from the BF_3 group to carbocationic atom C2 occurs, generating BF_2-bound fluorohydrin **36** (4.8 kcal/mol). This has a relative free energy similar to that of the starting reactive complex. Compound **36** can generate reaction product **38-N** through a two-step sequence involving fluoride transfer from C2 to the OBF_2 group and boryl migration (via TS **37**). The energy barrier of this reaction pathway (33.8 kcal/mol) is also higher.

In the routes in which the epoxide ring opening occurs at C2−O, boryl migration seems to be implicated. Our attempts to locate a mechanism that involves the shift of H_a from C_1 to C_2 were unsuccessful. This demonstrates that the BMIDA group can migrate easily because of the tetra-coordinated B atom.

Rupture of the C1−O Bond. Both *trans*-**31**-BF_3 and *cis*-**31**-BF_3 can undergo a concerted rearrangement through the *anti* (with the C2−O bond rotating toward H_a) and *syn* routes (with the C2−O bond rotating toward the BMIDA group) via TSs **39** and **42** to generate **38-N** and **38-X**, respectively (Figure 8). In TSs **39** and **42** the C2−H_c and C2−H_b bonds, respectively, are almost aligned with the vacant *p*-orbital of C1. TS **39** (34.2 kcal/mol) has a lower relative free energy than TS **42** (36.3 kcal/mol), but the energy barrier for the latter is lower (31.7 kcal/mol).

DOI: 10.1021/acs.joc.7b01096
J. Org. Chem. 2017, 82, 5917−5925

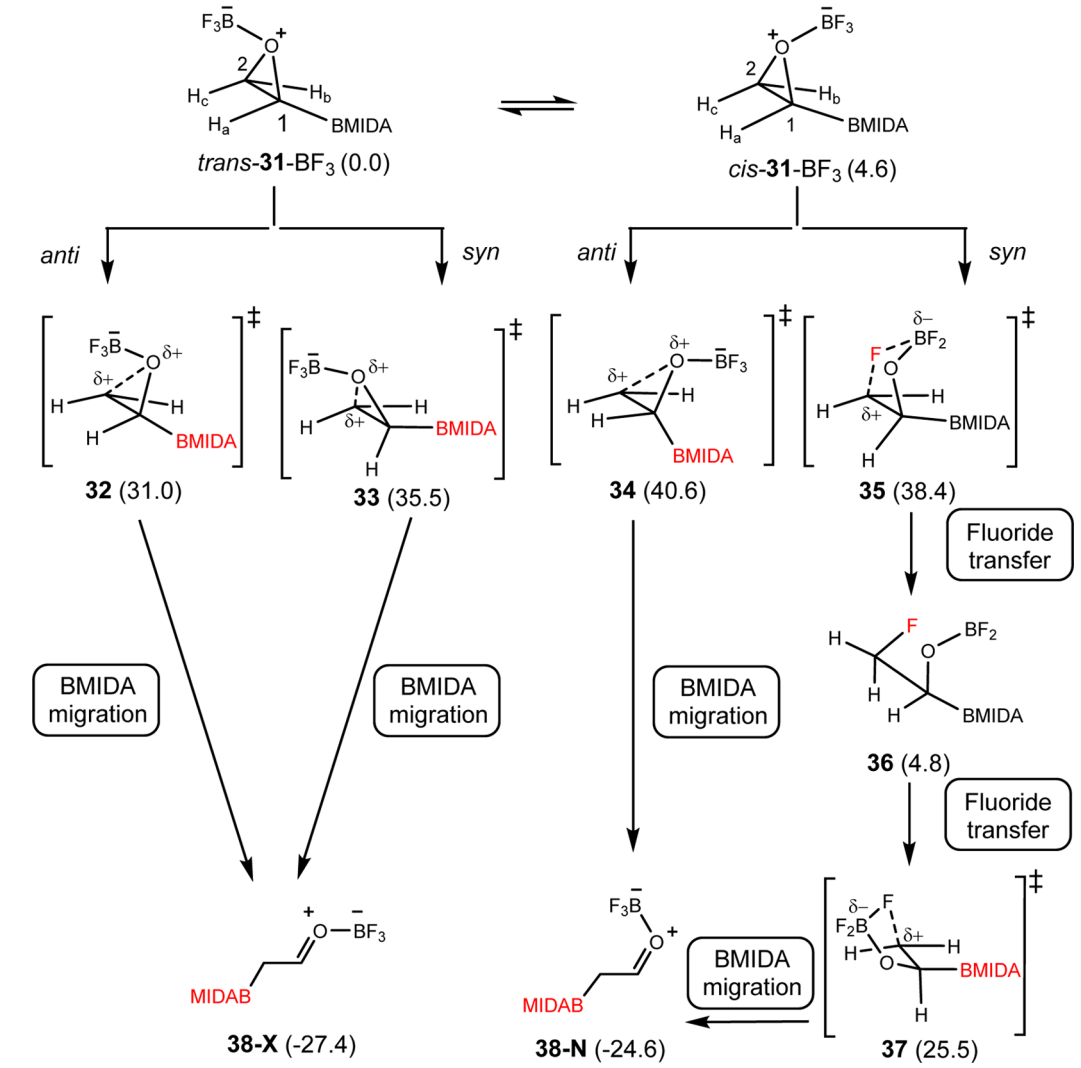

Figure 7. Reaction pathways of the rearrangement of the BF_3-coordinated oxiranyl MIDA boronate with rupture of the C2−O bond. Relative Gibbs free energies in DCM are given in parentheses (in kcal/mol).

Complexes *trans*-**31**-BF_3 and *cis*-**31**-BF_3 can also undergo a stepwise mechanism through the *syn* and *anti* pathways via TSs **40** and **41**, to generate intermediate BF_2-bound fluorohydrin compounds **43** and **44**, respectively. These mechanisms involve the fluoride transfer from the BF_3 group to the incipient carbocation at C1. TS **40** (31.0 kcal/mol) has a higher energy barrier than TS **41** (26.2 kcal/mol), and in both TSs a fluorine atom of the BF_3 group is in a favorable position to interact with C1 (C1−F = 2.27 Å in TS **40** and 2.40 Å in TS **41**). In the second step of the mechanism, compounds **43** and **44** undergo fluoride transfer and then H_b and H_c migration to generate **38-N** through TSs **45** and **46**, respectively. For the *anti* pathway, the hydride migration shows a slightly lower energy barrier (25.2 kcal/mol for TS **46**) than the first step.

The most-favorable mechanism for the rearrangement of BF_3-bound **31** (also displayed in Figure 9) involves fluoride transfer (through TS **41**) to give a BF_2-bound fluorohydrin compound (**44**). Then, fluoride transfer from C1 to the OBF_2 group and hydrogen migration occur (through TS **46**) to yield the final BF_3-coordinated α-boryl aldehyde product (**38-N**). The energy barriers for such a reaction are considerably higher than those calculated for the most-favorable mechanisms of BF_3-coordinated **1** and **24**, which explains the lack of the reactivity for **31**.[16] The larger activation barriers are attributed to the absence of the resonance contribution, which is reflected in the redistribution of the charges on the TSs (See the Supporting Information).

■ CONCLUSIONS

A detailed theoretical study on the mechanism of the BF_3-promoted rearrangement of 2- and 1-phenyl substituted and unsubstituted oxiranyl MIDA boronates was carried out using density functional theory in DCM. For each starting reactive, several pathways were investigated.

It was found that the most favorable pathway for the rearrangement of 2- and 1-phenyl oxiranyl MIDA boronates (**1** and **24**, respectively) takes place through a two-step mechanism involving (i) ring opening of C−O bond and C1−C2 rotation to form a carbocation intermediate and (ii) migration of BMIDA (for reaction of **1**) and hydride (for reaction of **24**), both leading to the same product, α-boryl aldehyde **14-X**. These mechanisms are in agreement with the experimental

DOI: 10.1021/acs.joc.7b01096
J. Org. Chem. 2017, 82, 5917−5925

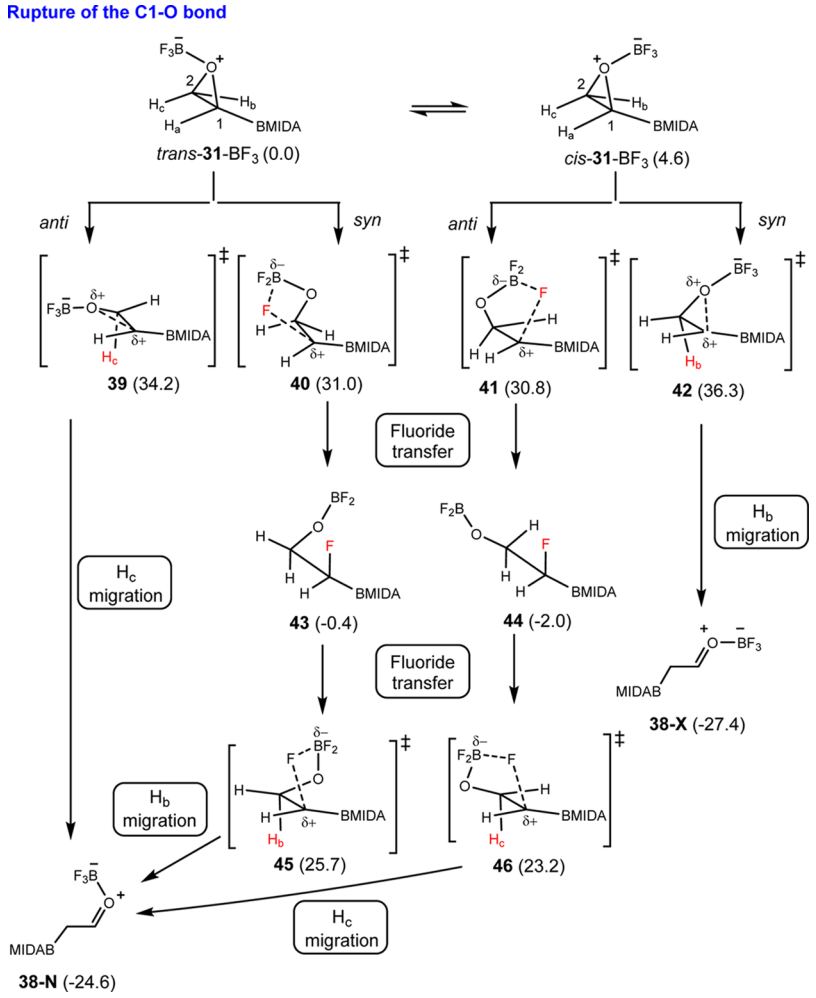

Figure 8. Reaction pathways of the rearrangement with rupture of the C2−O bond of the BF_3-coordinated oxiranyl MIDA boronate. Relative Gibbs free energies in DCM are given in parentheses (in kcal/mol).

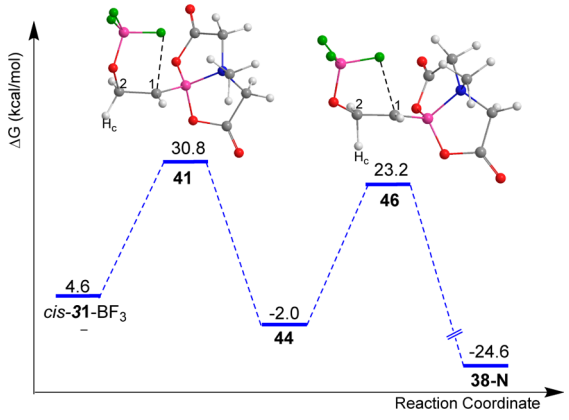

Figure 9. Reaction profile for the most-favorable pathway of BF_3-promoted rearrangement of oxiranyl MIDA boronate (**31**). Optimized geometries of the TSs **41** and **46** are shown.

results. In both pathways, the ring opening is the rate-determining step (the first step), and the cleavage of the bond between the oxygen and carbon atom attached to phenyl is energetically favored because the positive charge on the generated carbocation is delocalized and thus, stabilized by the resonance effect.

The calculations support that in the second step of the rearrangement of **1**, the BMIDA group migrates easily from intermediate carbocation **6** through TS **10**, because of the electron-rich nature of its sp^3-hybridized boron center.

In the second step of the rearrangement of **24**, H_b and H_c are equally well-positioned to shift, but rotation of C1−C2 toward the C1−O approaching the BMIDA group occurs through TS **30** to release the steric hindrance.

The experimentally observed regioselectivities are mainly dominated by electronic effects, although steric effects are also significant and determine the most favorable pathway.

The experimental lack of reactivity of BF_3-coordinated **31** could be explained through the higher energy barrier, which is mainly attributed to the absence of resonance effect. Interestingly, the most energetically favorable mechanism computed for BF_3-coordinated **31** involves a fluoride transfer to afford a BF_2-bound fluorohydrin intermediate (**44**), which undergoes fluoride transfer from C1 to the OBF_2 group and hydrogen migration to yield α-boryl aldehyde (**38-X**).

This study not only provides insight into the mechanism for the rearrangement of the BF_3-promoted oxiranyl MIDA boronates, but also demonstrates that the preferred reaction pathway is strongly dependent on the substrate structure. This should be taken into account to extend the scope of these novel compounds.

DOI: 10.1021/acs.joc.7b01096
J. Org. Chem. 2017, 82, 5917−5925

■ ASSOCIATED CONTENT

Supporting Information

The Supporting Information is available free of charge on the ACS Publications website at DOI: 10.1021/acs.joc.7b01096.

Additional computational results and supplementary computational data, such as the energies and Cartesian coordinates of stationary points (PDF)

■ AUTHOR INFORMATION

Corresponding Authors

*E-mail: vallejos.marga@gmail.com

*E-mail: pellegrinet@iquir-conicet.gov.ar.

Notes

The authors declare no competing financial interest.

■ ACKNOWLEDGMENTS

We thank CONICET and ANPCyT. M. M. V. thanks UNNE, and SECYT-UNNE. S. C. P. thanks UNR.

■ REFERENCES

(1) Gorzynski Smith, J. *Synthesis* **1984**, *1984*, 629−656.

(2) Shi, C.; Ren, C.; Zhang, E.; Jin, H.; Yu, X.; Wang, S. *Tetrahedron* **2016**, *72*, 3839−3843.

(3) Saddique, F. A.; Zahoor, A. F.; Faiz, S.; Naqvi, S. A. R.; Usman, M.; Ahmad, M. *Synth. Commun.* **2016**, *47*, 1−38.

(4) Krishnan, K. K.; Thomas, A. M.; Sindhu, K. S.; Anilkumar, G. *Tetrahedron* **2016**, *72*, 1−16.

(5) Shi, Y., Organocatalytic Oxidation. Ketone-Catalyzed Asymmetric Epoxidation of Alkenes and Synthetic Applications. In *Modern Oxidation Methods*; Bäckvall, J.-E., Ed.; Wiley-VCH Verlag GmbH & Co. KGaA: Weinheim, Germany, 2010; pp 85−115 (DOI: 10.1002/9783527632039.ch3).

(6) Lane, B. S.; Burgess, K. *Chem. Rev.* **2003**, *103*, 2457−2474.

(7) Díez, D.; Nuñez, M. G.; Antón, A. B.; Garcia, P.; Moro, R. F.; Garrido, N. M.; Marcos, I. S.; Basabe, P.; Urones, J. G. *Curr. Org. Synth.* **2008**, *5*, 186−216.

(8) George, P.; Bock, C. W.; Glusker, J. P. *J. Phys. Chem.* **1992**, *96*, 3702−3708.

(9) Coxon, J. M.; Maclagan, R. G. A. R.; Rauk, A.; Thorpe, A. J.; Whalen, D. *J. Am. Chem. Soc.* **1997**, *119*, 4712−4718.

(10) Coxon, J. M.; Thorpe, A. J.; Smith, W. B. *J. Org. Chem.* **1999**, *64*, 9575−9586.

(11) Bhatia, K. A.; Eash, K. J.; Leonard, N. M.; Oswald, M. C.; Mohan, R. S. *Tetrahedron Lett.* **2001**, *42*, 8129−8132.

(12) Ranu, B. C.; Jana, U. *J. Org. Chem.* **1998**, *63*, 8212−8216.

(13) Uno, B. E.; Gillis, E. P.; Burke, M. D. *Tetrahedron* **2009**, *65*, 3130−3138.

(14) Knapp, D. M.; Gillis, E. P.; Burke, M. D. *J. Am. Chem. Soc.* **2009**, *131*, 6961−6963.

(15) Hussain, N.; Hussain, M. M.; Carroll, P. J.; Walsh, P. J. *Chem. Sci.* **2013**, *4*, 3946−3957.

(16) He, Z.; Yudin, A. K. *J. Am. Chem. Soc.* **2011**, *133*, 13770−13773.

(17) Li, J.; Burke, M. D. *J. Am. Chem. Soc.* **2011**, *133*, 13774−13777.

(18) St. Denis, J. D.; He, Z.; Yudin, A. K. *Org. Biomol. Chem.* **2012**, *10*, 7900−7902.

(19) He, Z.; Zajdlik, A.; St. Denis, J. D.; Assem, N.; Yudin, A. K. *J. Am. Chem. Soc.* **2012**, *134*, 9926−9929.

(20) He, Z.; Zajdlik, A.; Yudin, A. K. *Dalton Trans.* **2014**, *43*, 11434−11451.

(21) He, Z.; Zajdlik, A.; Yudin, A. K. *Acc. Chem. Res.* **2014**, *47*, 1029−1040.

(22) Zajdlik, A.; He, Z.; St Denis, J. D.; Yudin, A. K. *Synthesis* **2014**, *46*, 445−454.

(23) Bai, J.; Burke, L. D.; Shea, K. J. *J. Am. Chem. Soc.* **2007**, *129*, 4981−4991.

(24) St. Denis, J. D.; Lee, C. F.; Yudin, A. K. *Org. Lett.* **2015**, *17*, 5764−5767.

(25) Shiroodi, R. K.; Koleda, O.; Gevorgyan, V. *J. Am. Chem. Soc.* **2014**, *136*, 13146−13149.

(26) Coxon, J. M.; Thorpe, A. J. *J. Org. Chem.* **2000**, *65*, 8421−8429.

(27) Fraile, J. M.; Mayoral, J. A.; Salvatella, L. *J. Org. Chem.* **2014**, *79*, 5993−5999.

(28) Zhao, Y.; Truhlar, D. G. *J. Phys. Chem. A* **2004**, *108*, 6908−6918.

(29) Vallejos, M. M.; Grimblat, N.; Pellegrinet, S. C. *RSC Adv.* **2014**, *4*, 36385−36400.

(30) Vallejos, M. M.; Pellegrinet, S. C. *RSC Adv.* **2015**, *5*, 70147−70155.

(31) Nacereddine, A. K.; Layeb, H.; Chafaa, F.; Yahia, W.; Djerourou, A.; Domingo, L. R. *RSC Adv.* **2015**, *5*, 64098−64105.

(32) Marenich, A. V.; Cramer, C. J.; Truhlar, D. G. *J. Phys. Chem. B* **2009**, *113*, 6378−6396.

(33) Hratchian, H. P.; Schlegel, H. B. *J. Chem. Phys.* **2004**, *120*, 9918−9924.

(34) Hratchian, H. P.; Schlegel, H. B. *J. Chem. Theory Comput.* **2005**, *1*, 61−69.

(35) Page, M.; McIver, J. W. *J. Chem. Phys.* **1988**, *88*, 922−935.

(36) Page, M.; Doubleday, C.; McIver, J. W. *J. Chem. Phys.* **1990**, *93*, 5634−5642.

(37) Wiberg, K. B. *Tetrahedron* **1968**, *24*, 1083−1096.

(38) Glendening, E. D.; Weinhold, F. *J. Comput. Chem.* **1998**, *19*, 610−627.

(39) Weinhold, F. *J. Comput. Chem.* **2012**, *33*, 2440−2449.

(40) Frisch, M. J. T., G. W; Schlegel, H. B.; Scuseria, G. E.; Robb, M. A.; Cheeseman, J. R.; Scalmani, G.; Barone, V.; Mennucci, B.; Petersson, G. A.; Nakatsuji, H.; Caricato, M.; Li, X.; Hratchian, H. P.; Izmaylov, A. F.; Bloino, J.; Zheng, G.; Sonnenberg, J. L.; Hada, M.; Ehara, M.; Toyota, K.; Fukuda, R.; Hasegawa, J.; Ishida, M.; Nakajima, T.; Honda, Y.; Kitao, O.; Nakai, H.; Vreven, T.; Montgomery, J. A., Jr.; Peralta, J. E.; Ogliaro, F.; Bearpark, M.; Heyd, J. J.; Brothers, E.; Kudin, K. N.; Staroverov, V. N.; Kobayashi, R.; Normand, J.; Raghavachari, K.; Rendell, A.; Burant, J. C.; Iyengar, S. S.; Tomasi, J.; Cossi, M.; Rega, N.; Millam, N. J.; Klene, M.; Knox, J. E.; Cross, J. B.; Bakken, V.; Adamo, C.; Jaramillo, J.; Gomperts, R.; Stratmann, R. E.; Yazyev, O.; Austin, A. J.; Cammi, R.; Pomelli, C.; Ochterski, J. W.; Martin, R. L.; Morokuma, K.; Zakrzewski, V. G.; Voth, G. A.; Salvador, P.; Dannenberg, J. J.; Dapprich, S.; Daniels, A. D.; Farkas, Ö.; Foresman, J. B.; Ortiz, J. V.; Cioslowski, J.; Fox, D. J. *Gaussian 09, Revision D.01*, Gaussian, Inc.: Wallingford CT, 2009.

(41) The terms *cis* and *trans* correspond to the position of BF_3 group relative to the BMIDA moiety.

(42) *Exo*/*endo* labeled with "X"/"N" indicate that the BF_3 group is placed out/into the C1−C2 bond.

(43) He, Z.; Trinchera, P.; Adachi, S.; St. Denis, J. D.; Yudin, A. K. *Angew. Chem., Int. Ed.* **2012**, *51*, 11092−11096.

(44) Coxon, J. M.; Hartshorn, M. P.; Lewis, A. J.; Richards, K. E.; Swallow, W. H. *Tetrahedron* **1969**, *25*, 4445−4448.

(45) Blackett, B. N.; Coxon, J. M.; Hartshorn, M. P.; Richards, K. E. *Tetrahedron* **1969**, *25*, 4999−5005.

(46) Coxon, J. M.; Hartshorn, M. P.; Muir, C. N. *Tetrahedron* **1969**, *25*, 3925−3933.

(47) Blackett, B. N.; Coxon, J. M.; Hartshorn, M. P.; Jackson, B. L. J.; Muir, C. N. *Tetrahedron* **1969**, *25*, 1479−1487.

(48) Islas-González, G.; Puigjaner, C.; Vidal-Ferran, A.; Moyano, A.; Riera, A.; Pericàs, M. A. *Tetrahedron Lett.* **2004**, *45*, 6337−6341.

(49) Cresswell, A. J.; Davies, S. G.; Lee, J. A.; Roberts, P. M.; Russell, A. J.; Thomson, J. E.; Tyte, M. J. *Org. Lett.* **2010**, *12*, 2936−2939.

DOI: 10.1021/acs.joc.7b01096
J. Org. Chem. 2017, 82, 5917−5925